13th International Symposium on Particle Image Velocimetry – ISPIV 2019
Munich, Germany, July 22-24, 2019

Large-scale Stereo-PIV measurement of the flow inside an urban street canyon in outdoor conditions

S. Herpin[1,3*], D. Heitz[2,4], P. Loisel [2], P. Georgeault[2]

[1] EPHOR, AGROCAMPUS OUEST, 49045 Angers, France

[2] Irstea, UR OPAALE, F-35044 Rennes Cedex, France

[3] IRSTV, FR CNRS 2488, 44321 Nantes Cedex 3, France

[4]Inria, Fluminance group, Campus universitaire de Beaulieu, F-35042 Rennes Cedex, France

[*] sophie.herpin@agrocampus-ouest.fr

Abstract

More than 50% of the worlwide population are city dwellers, this percentage reaching up to 80% in Europe. Urban heat island effect and global climate change are therefore expected to put the population at stress, with well-being or health related issues. In this contibution, we propose to investigate the wind field in a model urban environment in outdoor conditions. Atmospheric flows in urban environments are complex (3D and turbulent). Field measurement techniques such as particle image velocimetry (PIV) can bring valuable information, in comparison with usual pointwise sensors such as sonic anemometers. In this contribution, large scale stereoscopic PIV measurements are undertaken in a 2m by 2m cross section of an outdoor Canyon street at the 1 : 5 scale. Handling fluctuating wind conditions, achieving sufficient seeding, and coping with natural light are important challenges for the PIV technique in outdoor environments. Several datasets could be acquired with a good global datarate, under various conditions of wind directions and convection regimes. The analysis of mean velocity fields reveals the influence of thermal effects near the building walls on the flowfield. The conditions of appearance of a windwise vortex in the cross section of the street are also discussed.

1 Introduction

In a context of worldwide urban densification and global climate change, characterizing the urban microclimate in city centers is of primary importance. In particular, the wind at street level plays a key role in the transport of heat and particles. Field experiments benefit from real climatic outdoor conditions. However, results obtained with in-situ experiments in real cities (Louka et al., 2001; Rotach et al., 2005) are difficult to generalize due to the heterogeneous and very large range of urban shapes. A few studies at reduced but moderate scale (typically ranging from 1:2 to 1:10) in outdoor conditions have considered more canonical geometries, such as array of large cubes to model suburban areas (Inagaki and Kanda, 2008), or canyon streets to model city centers (Idczak et al., 2007). In outdoor climatic studies, the wind information is usually retrieved with single-point wind sensors such as sonic anemometers and is thus fairly limited.
In order to get a comprehensive view of the complex 3D and turbulent flowfield in urban areas, field measurement techniques such as particle image velocimetry (PIV) are required. PIV is a well established measurement technique in lab conditions. Large-scale PIV with field of view of several meter square has been achieved in indoor conditions (Bosbach et al., 2009). However, its extension to outdoor conditions remains a real challenge. Two recent studies have used planar 2D2C PIV at nightime, to study the atmospheric surface layer during winter season using natural snowfall (Toloui et al., 2014), or during summer time using smoke seeding in a cube array facility representing a suburban area (Takimoto et al., 2011). These pioneering studies point out the difficulty to handle the fluctuating wind-direction inherent to outdoor experiments with 2D2C PIV, because of out-of-plane motions. Another severe limitation is linked to the seeding : it is difficult to achieve homogeneous and sufficient seeding in outdoor conditions using artificial tracers.
In the present contribution, we investigate the wind-field in a city center environnement in typical summertime climatic conditions, in order to get a better understanding of the role of wind in the mitigation of the

Figure 1: Canyon Street of Agrocampus Ouest, Angers, France

urban heat island effect. In order to do so, we propose to stretch the boundaries of PIV by implementing large-scale-PIV in outdoor conditions with stereoscopic reconstruction, to better handle out-of-plane motions. The experiments are realized in a model urban environment at the 1:5 scale. 2D3C velocity fields are obtained in a 2 m $\times$ 2 m cross-section of an urban street canyon, both at day and night time.

2 Experimental Details

2.1 The Canyon Street Facility

The experiments were carried out in the model Canyon street facility of Agrocampus Ouest, located in Angers, France (47°28′ North, 0°36′ West). The street is North-South oriented, orthogonal to the prevailing winds. The street has nominal dimensions of 16m in length, 2m in width, and is flanked on both sides by buildings with a height H=2m (Fig. 1). The ground is covered with asphalt and the walls are made of concrete, to be representative of urban construction materials. The aspect ratio of the street, defined as the ratio of the buiding height to the street width is 1, resulting in a regular Canyon street. The geometrical scaling factor of Agrocampus Ouest Canyon street is 1 : 5, taking 10m as the full-scale reference building height.

2.2 Flow conditions during the experiment

The measurements were realized in september 2018 from the 11th evening (17:00 UTC) to the 12th early-night (20:00 UTC), under sunny and warm conditions. Sunrise was at 05:30 and sunset at 18:20 (UTC). The wind speed, direction, and air-temperature outside the street were measured with a meteorological mast reaching up to 5.4 m from the ground, equipped with a 2D sonic anemometer and a PT100 sensor. The climatic variables were measured at a frequency of 0.1Hz, and a sliding average was operated and recorded every 10min. The wind was weak, evolving from a very low wind speed (< 1 m/s) with fluctuating orientation on the 11th to a quite low wind speed (< 2 m/s) with a north north-west orientation from the 12th afternoon (Fig. 2(a)).
The Richardson number, which characterizes the importance of the buoyancy forces in respect with the inertial forces, can be computed as :

$$Ri = -gH\frac{(T_p - T_0)}{T_0}\frac{1}{U_0^2} \tag{1}$$

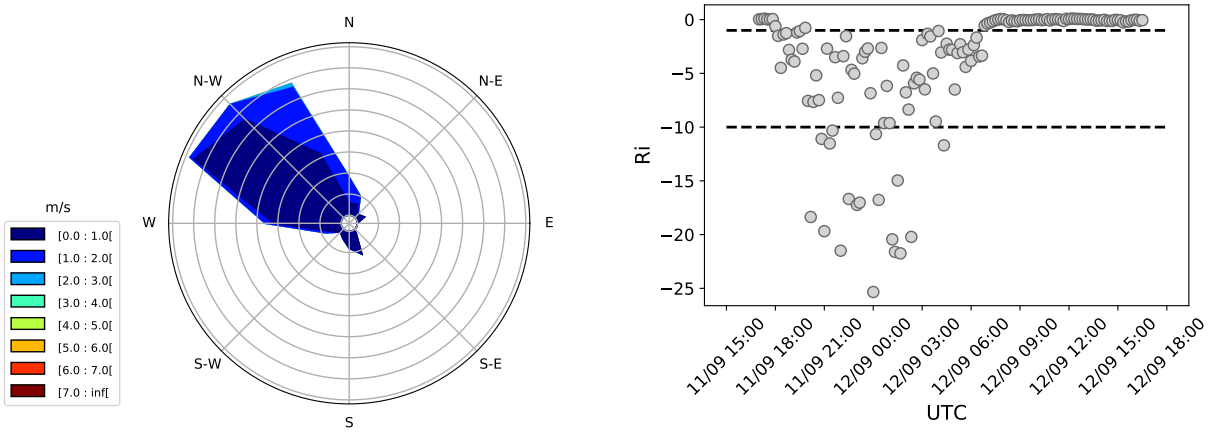

(a) Wind-Rose

(b) Richardon Number

Figure 2: Flow conditions during PIV experiments. In subfigure (b), the dashed lines represents the boundaries of forced ($Ri = -1$) and natural convection ($Ri = -10$). In between, the flow regime is mixed convection.

Where :

- T_p is the wall temperature of the Canyon Street, measured with Pt100 sensors, taken as the average temperature between the west and the east wall
- T_0 is the air temperature in the free-stream outside the street (measured with the meteorological mast)
- H is the height of the street walls (2m)
- U_0 is the wind speed in the free stream outside the street (measured with the meteorological mast)

When the Richardson number is close to zero, the flow conditions are neutral, and the flow regime is forced convection. When the Richardson nunber is above zero, the flow is stable. When the Richardson number is negative, the flow conditions are unstable, with mixed convection when $-10 \leq Ri \leq -1$ and natural convection when $Ri \leq -10$. The Richardson number during the PIV experiment is reported in figure 2(b). Overall, the flow conditions were neutral during daytime, and unstable at nightime, varying between mixed and natural convection depending on the intensity of the wind speed, and leaning towards natural convection at midnight. Overall, the climatic conditions were favourable to the appearance of an urban heat-island effect.

2.3 Stereo-PIV setup

The flowfield inside a 2 m $\times$ 2 m cross section of the Canyon street, located at 5m from the South end of the street, was investigated using Stereoscopic Particle Image Velocimetry. Two cameras Imager sCMOS (2560 px $\times$ 2160 px) were equipped with 35 mm focal length lenses and arranged in a stereoscopic configuration (19.2°) to image the field of view (dimensions 2022 mm $\times$ 2386 mm) with a spatial resolution of about 1.1 px/mm (Fig. 3(a)). A calibration target was used to back-project the image plane into the object plane and allow the stereoscopic reconstruction (Fig. 3(b)). The measurement plane was illuminated using a 200 mJ laser (EverGreen from Quantel), shaped into a 25 mm thick laser sheet (Fig. 4(a)). Specific filters centered on the laser wavelength were fitted on the cameras to remove background light noise. The air inside the canyon was seeded with Helium-Filled soap bubbles (nominal diameter 300μm). During the period of study which extended during 26 hours from the 11th of september evening to the 12th of september early night, 23 sets of 2000 image pairs were collected with an acquisition frequency of 12.5 Hz.

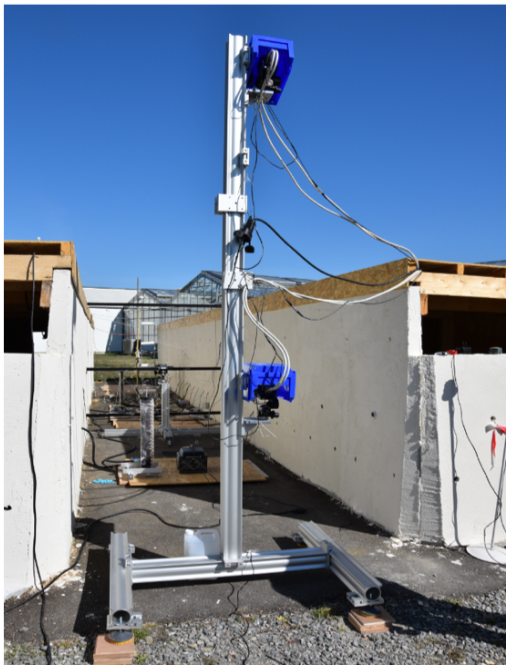

(a) Stereo-PIV setup arrangement

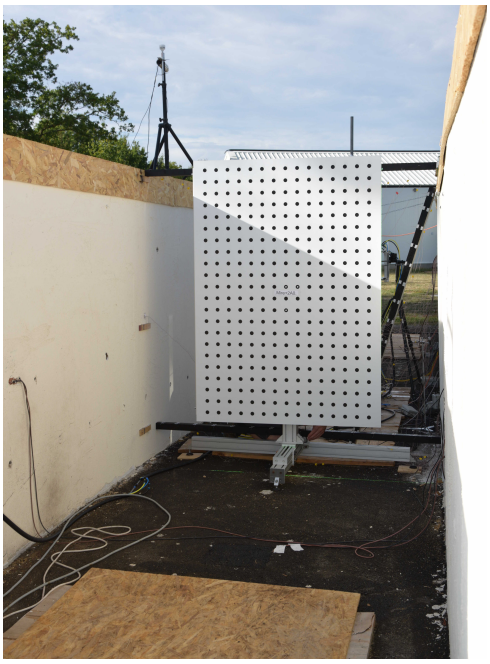

(b) calibration target

Figure 3: Stereo-PIV experiments in Agrocampus Ouest Street Canyon

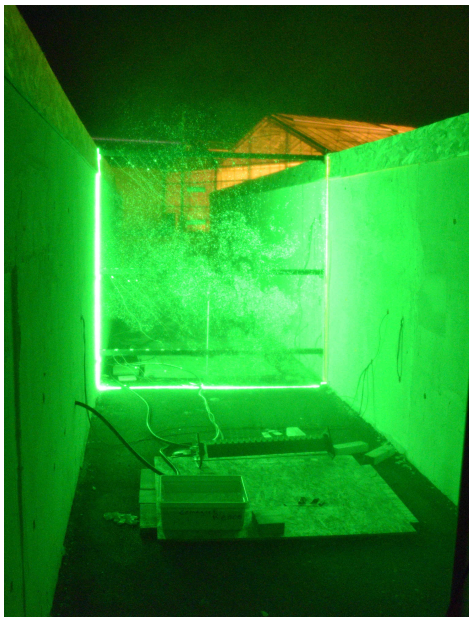

(a) laser sheet and seeding

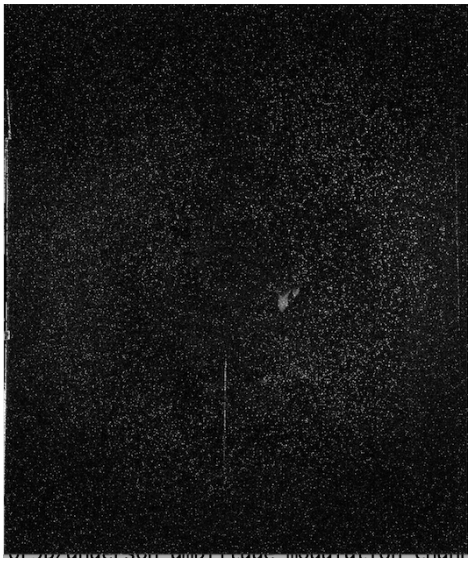

(b) Particule image from bottom camera

Figure 4: Laser sheet, seeding and particle images

2.4 Image Processing

The PIV data images were processed with the LaVision DaVis 10 software. A pre-processing (subtract the minimum intensity for each pixel position from all 2 000 consecutive images) was applied to the images to eliminate reflections. Then, cross-correlations were performed on image pairs in multiple passes, starting from an interrogation window size of 96×96 pixels with 50% overlap followed with three iterations for a final interrogation window size of 96×96 pixels with 75% overlap. During this process, vectors were deleted if the correlation peak ratio was strictly less than 0.5. As a post-processing, spurious vectors were detected with the universal outlier detection approach of Westerweel and Scarano (2005), removing vector if the residual was > 2.0 pixels and reinserting it if the residual was < 3.0 pixels. This filter was applied in region of 5×5 vectors and empty spaces were filled-up via linear interpolation with a minimum number of four neighbouring vectors. The whole process took 17h of computational time for 2 000 image pairs.

The calibration was conducted with a home-made calibration target of size $2 \times$ A0 registered and mapped via a pinhole model to the image plane of both cameras. The self-calibration technique proposed by Wieneke (2005) was used to correct for the potential misalignments of the target with respect to the laser sheet.

3 Results

3.1 PIV quality : Valid Data Rate

The experiment is carried out in harsh conditions for PIV measurement technique : the field of view is large (2m*2m), and the outdoor environment impose flucuating wind conditions and short time of residence of the tracer inside the field of view. Following Takimoto et al. (2011), we analyze the Valid Data Rate (VDR), in order to assess the quality of each dataset:

$$VDR(x_i, z_j) = \frac{1}{N} \sum_{n=1}^{N} \varepsilon(x_i, z_j, n) \tag{2}$$

Where x_i and z_j are the x and z coordinate of the datapoint, N is the number of samples (velocity fields) in the dataset, and ε is a "flag" function taking the value of 1 for valid datapoint and 0 for non-valid datapoint. A global valid datarate (GVDR) can be computed by spatially averaging the VDR across all the field of view (1 value per dataset).

The GVDR was varying between 0.2 and 0.9 among the datasets, decreasing as the incoming wind was getting more fluctuating in direction. Indeed, the position of the seeding ramps could not be adapted during a dataset acquisition to ensure it was always placed upstream or at a suitable position. Another limiting factor was the very low wind-speed, which could reached down to 0.1 $\mathrm{m/s}$ (measured with the meteorological mast at 5.4 m from the ground) : the seeding ramps had to be placed quite close to measurement section, and switched-off just before the start of acquisition to avoid any interference with the flow ; in this case in was not possible to keep the tracer particles long enough in the measurement section and the acquisition was limited to 500 image pairs. With this limitation, satisfactory datarate could be achieved.
Finally, only the datasets with a global datarate above 0.8 were retained for further analysis (see table 1). The valid datasets are under north-west oblique wind conditions, with datasets closer to a west wind (282° - almost perpendicular to the street) or to a northen wind (347° - almost parallel to the street)). The Richardon number ranges from -7.28 (mixed close to natural convection) to -0.08 (neutral conditions) and allows the investigation of different flow regimes. As it can be seen the large out-of-plane motions with winds coming mainly from the North (347°) are well handled thanks to the stereoscopic configuration. One dataset was acquired during daytime (12/09/2018 07:20), which shows the ability of PIV to handle daylight, thanks to the optical filters on the cameras.

UTC	Wind speed (m/s)	Wind Dir. (°)	σ (°)	Ri	DataRate	Number samples
11/09/2018 20:30	0.18	291	11.81	-5.18	0.86	500
11/09/2018 21:50	0.16	300	47.58	-7.28	0.87	500
12/09/2018 07:20	0.48	282	28.28	-0.16	0.82	2000
12/09/2018 19:10	1.2	336	24.82	-0.09	0.82	2000
12/09/2018 19:50	1.14	347	33.8	-0.08	0.87	2000

Table 1: Datasets with a satisfactory global Valid Data Rate.σ is the standard deviation of the wind direction.

The spatial distribution of valid datarate (VDR) is shown in figure (5), for two datasets with almost perpendicular (a) and parallel (b) incoming wind directions, with respect to the main street axis. The pattern is actually quite similar among all datasets. An excellent datarate is achieved over most of the field of view, even for incoming winds parallel to the street main axis (corresponding to the out-of-plane direction for PIV). A small radial decrease is observed towards the boundaries of the velocity field. This was explained by the decrease of light on the edges of the camera CCD array due the presence of optical filters on the camera. The velocity field in the vicinity of the vertical walls is still well resolved, thanks to the white painting of the walls which reflects back the laser light. The pattern obtained is very different to that of Takimoto et al. (2011), who obtained a low datarate region in the center of the street. The good valid datarate obtained across the street cross-section matches well with our interest in the urban climate inside the street.

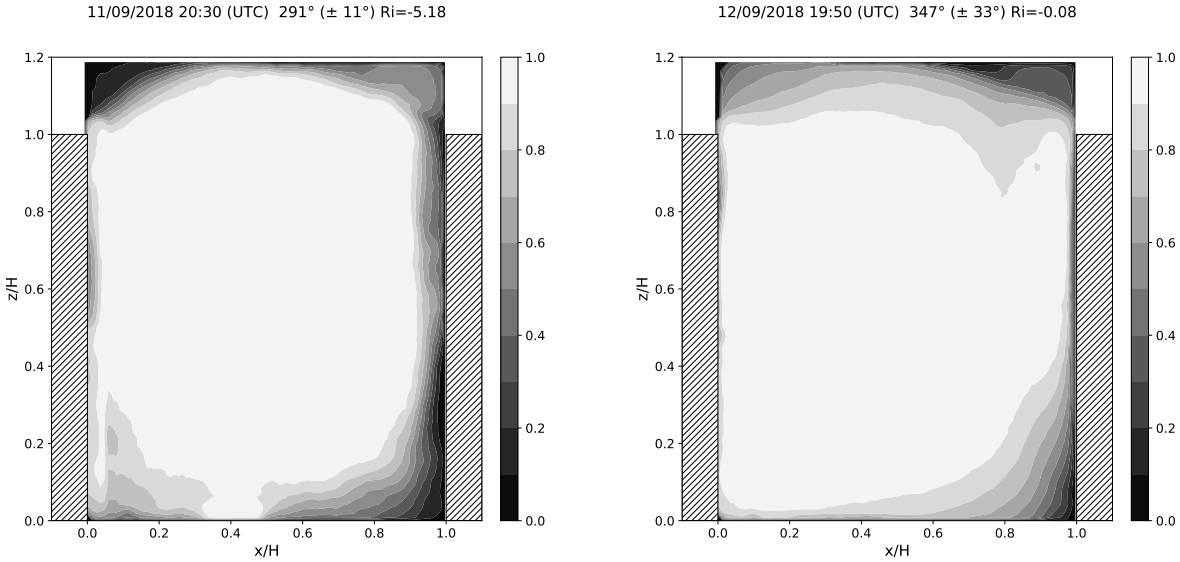

(a) (b)

Figure 5: Spatial Distribution of Valid Data Rate

3.2 Mean Velocity Fields

The mean velocity fields for the different flow conditions are shown in figure 6.
The flowfields in subfigures (c) and (d) are in the forced convection regime, close to neutrality ($Ri = -0.09$ and -0.08). With the incoming wind coming from 336° and 347° respectively, the main flow inside the street is predominantly parallel to the street axis (corresponding to an out-of-plane motion). The weak wind component coming from the west gives rise to a secondary flow with a clockwise rotating motion inside the test section.
In subfigure (b), the flow is coming more from the west (282°), and the out-of-plane velocity is reduced. A weak clockwise rotating motion is also visible. The flow is in the mixed convection regime ($Ri = -0.16$). A vertical boundary layer developping along the western wall (heated up by the sun from the east in the morning) is visible, and strenghten the vortical motion on this side on the street.
Finally, subfigure (a) shows a case of mixed convection with stronger thermal effects ($Ri = -5.18$), with west/north-west incoming wind (291°). A main clockwise vortex in the upper half of the street is visible, but thermal convection occuring on the eastern wall at early night induces a counter-rotating vortex.
The clockwise rotating vortex can be observed in the various datasets for different wind direction, mostly oblique (north-west), and sometimes leaning to west or north direction. Previous studies of canyon streets in wind-tunnels (Kastner-Klein et al., 2004) with a purely perpendicular wind have shown the existence of such a wind-wise vortex. We see here that it is maintained also in conditions of oblique and fluctuating wind. In our datasets, the vortex is sometimes not fully closed, especially on top of the street. This is

visible in subfigures (b) and (d), where the wind velocity component perpendicular to the street is the largest ($U_{x,\infty}$=0.47m/s, measured at 5.4m from the ground outside the street). This may be due to a detachment of the flow occuring on the upstream corner of the left-handside building, which is not measured here but sometimes reported in the litterature (Garcia Sagrado et al., 2002). For winds with a weaker perpendicular velocity component (subfigures (a) and to a less extent (d)), the vortex exhibits a more closed shape at the top of the street.

4 Conclusion

Large-scale stereoscopic PIV measurements were undertaken inside an outdoor Canyon street in order to get a better understanding on the flowfield in urban environments. The experiments were realized under sunny, warm, and low wind conditions, favourable to the appearance of a heat-island effect. Handling fluctuating wind direction and achieving good seeding was very challenging in outdoor environment. Several datasets could be acquired with a good datarate under various conditions of wind, convection regime, and both at day and nightime. In the mixed convection regime, thermal effects are visible on the east and west walls, depending on the time of the day. These effects either strengthen or weaken the main vortex appearing inside the test section for incoming winds with a component perpendicular to the street.

Acknowledgements

This collaborative work between Agrocampus Ouest and IRSTEA benefited from financial support of Universite Bretagne Loire (starter young researcher grant (5k€)). The authors wish to thank Dominique Lemesle, laboratory technician at Agrocampus Ouest, for technical support with climatic measurements during the experiment.

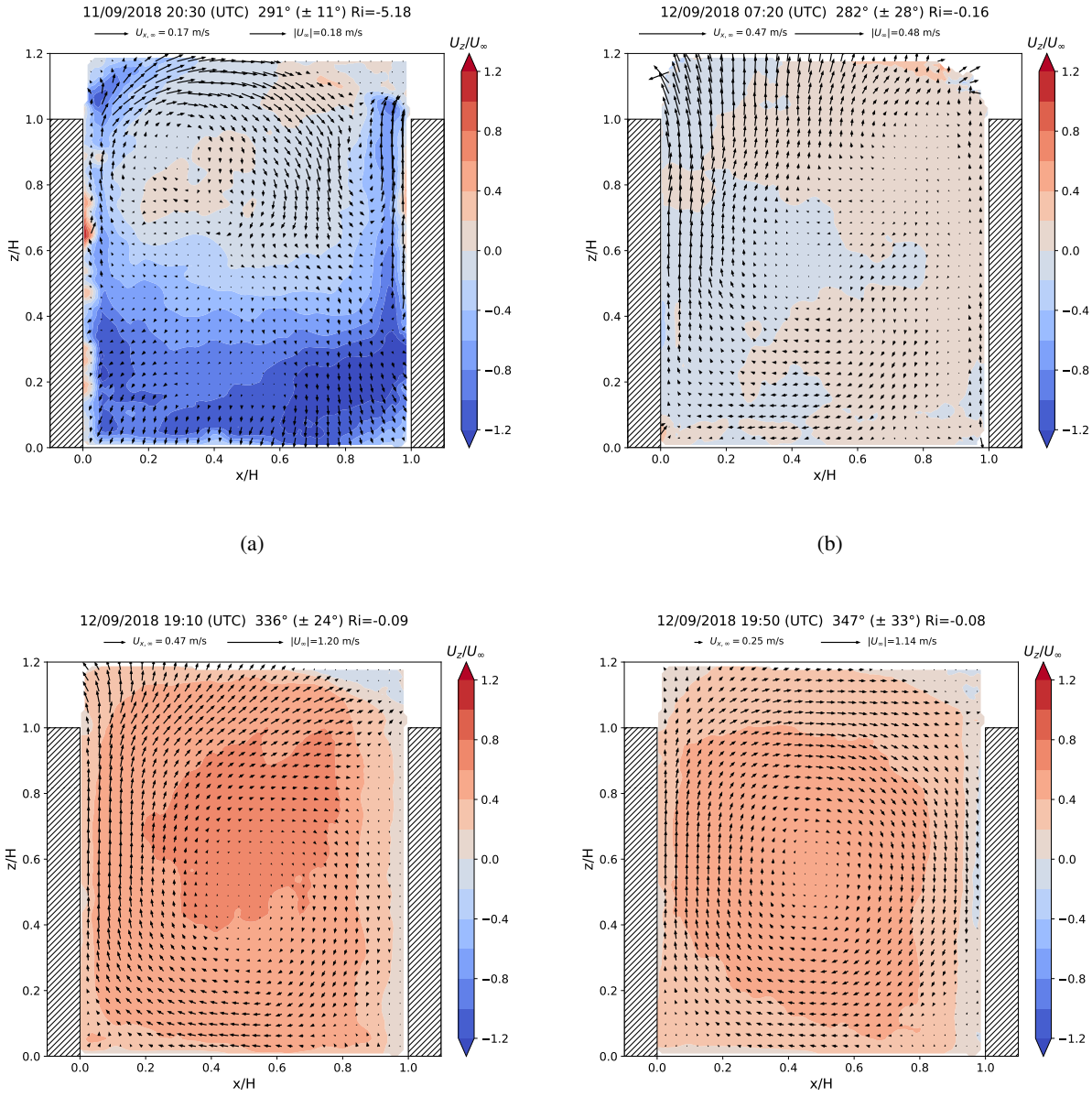

Figure 6: Mean Velocity Fields in the XZ section of the Canyon street. Only one in every three vectors is shown in both directions.The west direction is on the left handside, and the east direction to the right.

References

Bosbach J, Kühn M, and Wagner C (2009) Large scale particle image velocimetry with helium filled soap bubbles. *Experiments in Fluids* 46:539–547

Garcia Sagrado AP, van Beeck J, Rambaud P, and Olivari D (2002) Numerical and experimental modelling of pollutant dispersion in a street canyon. *Journal of Wind Engineering and Industrial Aerodynamics* 90:321–339

Idczak M, Mestayer P, Rosant JM, Sini JF, and Violleau M (2007) Micrometeorological Measurements in a Street Canyon during the Joint ATREUS-PICADA Experiment. *Boundary-Layer Meteorology* 124:25–41

Inagaki A and Kanda M (2008) Turbulent flow similarity over an array of cubes in near-neutrally stratified atmospheric flow. *Journal of Fluid Mechanics* 615:101

Kastner-Klein P, Berkowicz R, and Britter R (2004) The influence of street architecture on flow and dispersion in street canyons. *Meteorology and Atmospheric Physics* 87

Louka P, Vachon G, Sini JF, Mestayer P, and Rosant JM (2001) Thermal Effects on the Airflow in a Street Canyon – Nantes '99 Experimental Results and Model Simulation. Loutraki

Rotach MW, Vogt R, Bernhofer C, Batchvarova E, Christen A, Clappier A, Feddersen B, Gryning SE, Martucci G, Mayer H, Mitev V, Oke TR, Parlow E, Richner H, Roth M, Roulet YA, Ruffieux D, Salmond JA, Schatzmann M, and Voogt JA (2005) BUBBLE – an Urban Boundary Layer Meteorology Project. *Theoretical and Applied Climatology* 81:231–261

Takimoto H, Sato A, Barlow JF, Moriwaki R, Inagaki A, Onomura S, and Kanda M (2011) Particle Image Velocimetry Measurements of Turbulent Flow Within Outdoor and Indoor Urban Scale Models and Flushing Motions in Urban Canopy Layers. *Boundary-Layer Meteorology* 140:295–314

Toloui M, Riley S, Hong J, Howard K, Chamorro LP, Guala M, and Tucker J (2014) Measurement of atmospheric boundary layer based on super-large-scale particle image velocimetry using natural snowfall. *Experiments in Fluids* 55:1737

Westerweel J and Scarano F (2005) Universal outlier detection for PIV data. *Exp Fluids* 39:1096–1100

Wieneke B (2005) Stereo-PIV using self-calibration on particle images. *Exp Fluids* 39:267–280